Chinese Chemical Letters 31 (2020) 931–936

Contents lists available at ScienceDirect

Chinese Chemical Letters

journal homepage: www.elsevier.com/locate/cclet

Review

Recent progress of MXenes as the support of catalysts for the CO oxidation and oxygen reduction reaction

Yiying Zhang[a], Xilin Zhang[a], Cheng Cheng[b], Zongxian Yang[a,c,*]

[a] School of Physics, Henan Normal University, Xinxiang 453007, China
[b] College of Chemistry, Key Laboratory of Theoretical & Computational Photochemistry of Ministry of Education, Beijing Normal University, Beijing 100875, China
[c] National Demonstration Center for Experimental Physics Education (Henan Normal University), Xinxiang 453007, China

ARTICLE INFO

Article history:
Received 4 November 2019
Received in revised form 28 November 2019
Accepted 29 November 2019
Available online 5 December 2019

Keywords:
MXenes
Catalysis
Substrate material
CO oxidation
ORR

ABSTRACT

MXenes, the new family of two-dimensional (2D) transition metal carbides/nitrides, can serve as the substrate materials for the catalysts due to the large specific surface area, tunable electronic structures and thermal stability. The first 2D layered MXene, Ti_3C_2, was successfully obtained by selective etching of the A element from the MAX phases using hydrofluoric acid (HF) at room temperature in 2011. In this review, we summarize the preparation, structure of MXenes and discuss the recent progress in potential application of MXenes in catalysis, mainly in CO oxidation and oxygen reduction reaction (ORR), from the views of both experimental and theoretical investigations. The outlook of the major challenges and future directions on research of MXenes is also included.

1. Introduction

In the practical operation of proton exchange membrane fuel cells (PEMFCs), a little amount of CO contained in the hydrogen fuel could poison the anode, diminish the catalytic activity of electrocatalysts, and further cause the electrocatalysts degradation [1]. Therefore, it is necessary to remove the CO containment through efficient method like the CO oxidation reaction because the CO impurity could hardly avoid in the process of methanol and alcohol decomposition [2]. In the cathode of PEMFCs, the poor oxygen reduction reaction (ORR) catalytic performance in the cathode and low stability of the ORR electrocatalysts are the main obstacles for the development of fuel cells [3,4]. In the recent decades, the Pt/C catalysts showed the highest performance for ORR as the most active and widely-used electrocatalysts in the large-scale applications. However, there still remain some challenges for the Pt/C catalysts due to the scarcity and high cost of platinum and the corrosion of carbon supports [5,6]. Therefore, searching for the promising electrocatalysts with high stability, corrosion-resistant and high catalytic activity for CO oxidation and ORR are of great practical importance.

Since the discovery of graphene in 2004 by Novoselov [7], the two-dimentional (2D) materials have attracted tremendous interest in recent years due to their unique physical and chemical properties for the application in material science and catalysis. Other 2D materials beyond graphene such as black phosphorus (BP) [8], hexagonal boron nitride (h-BN) [9–11], transition metal dichalcogenides (TMDs) [12,13], oxides, early transition metal carbides and/or nitrides (MXenes) [14], *etc*., have also been prepared. The application of these 2D materials as an excellent support in the catalysis (such as water splitting [15–17], Li-O_2 batteries [18], hydrogen generation [19], hydrogen evolution reactions (HER) [20] and ORR [21]) has grown rapidly over the past years due to their unprecedented characteristics, such as containing the active sites or utilizing as the metal-free catalysts, possessing high specific surface area [22–24]. Besides, these materials could also be applied for the electromagnetic wave shielding [25], electrochemical energy storage [26], negative permittivity materials [27,28], and so on.

As a young member in the large 2D materials family, MXenes have attracted extensive attention worldwide due to the similar configuration to graphene [14,29], their rich surface chemistry, adjustable electronic structures and thermal stability [22]. The chemical formula of MXenes is $M_{n+1}X_nT_n$ (n = 1–3), in which M denotes the early transition metal elements, X represents C or/and N, T is the surface termination groups (usually O, OH and F, *etc*.). MXenes could be successfully achieved by selective etching the "A"

* Corresponding author at: School of Physics, Henan Normal University, Xinxiang 453007, China.
E-mail address: yzx@henannu.edu.cn (Z. Yang).

https://doi.org/10.1016/j.cclet.2019.12.010
1001-8417/

group layer from the MAX phases, where "M" represents early d transition metals, "A" represents the main groups IIIA and IVA sp-elements, and "X" represents C or/and N [30], normally using hydrofluoric acid (HF) or HF containing etchants at room temperature [31]. Furthermore, because of the active properties of the bare MXenes surface, the surface functional groups such as O, OH and F are always terminated on the MXenes depending on the etching agents and subsequent treatment [14,32,33]. Nevertheless, MXenes are always covered with OH or O groups when they are kept in water, which indicates that OH or O terminated groups are more stable, but the high-temperature annealing makes the OH functional groups convert into O group [34].

Since the first MXene, Ti_3C_2, was synthesized in 2011, MXenes have grown rapidly in the recent few years and more than 20 kinds of MXenes have been synthesized up to now, including Ti_2C, V_2C, Nb_2C, Mo_2C, $(Ti,V)_2C$, $(Ti,Nb)_2C$, Ti_3C_2, $Ti_3(C,N)_2$, Zr_3C_2, $(Ti,V)_3C_2$, $(Cr,V)_3C_2$, $(Mo_2Ti)C_2$, $(Cr_2Ti)C_2$, Ti_4N_3, Nb_4C_3, Ta_4C_3, $(Ti,Nb)_4C_3$, $(Nb,Zr)_4C_3$, $(Mo_2Ti_2)C_3$ [35]. Aside from the single and double transition metal carbides, numerous two-dimensional transition metal nitrides (such as Ti_4N_3) [36] and carbonitrides (such as Ti_3CN) [37] have also been discovered. And there were also many theoretical investigations for the intrinsic properties of transition metal nitrides [38–40]. MXenes and their composites could be widely used for their excellent electrical conductivity and excellent hydrophilicity as battery materials [34, 41–43], energy storage materials [35,44,45], and sensors [46–48] in several applications [49]. In addition, MXenes possess some desirable properties, such as the tunable surface properties and good mechanical stability [44], which make them suitable for being used as supports in the electrocatalysts [50–52], as shown in Fig. 1. Cheng *et al.* [53] developed the HER and oxygen evolution reaction (OER) bifunctional electrocatalysts, which utilized the Cr_2CO_2 supported Ni as the single atom catalysts (SACs) for the whole water splitting process and the overpotentials of HER and OER reached 0.16 and 0.46 V, respectively.

Many works have summarized the synthesis, properties, and potential applications (for example, photothermal conversion, energy storage, transparent conductors, and environmental remediation) of MXenes [14,54–56]. However, there were few investigations paid close attention to the catalytic properties of MXenes. In this review, we discuss mainly about the experimental and theoretical researches on MXenes. The summary and outlook of MXenes are also included. We mainly focus on the electrocatalytic properties of titanium carbide MXene and molybdenum carbide MXene because of their low-cost and high activity in ORR and CO oxidation.

2. The synthesis and crystal structure of MXenes

As noted above, the MXenes can be obtained by chemically and selectively etching the A elements (such as Al^{3+} or Si^{4+}) of the MAX phases at room temperature. The weakly-bonded A layer with M in MAX is the prerequisite for the selectively and chemically etching of A-element layer because the M—A bonds are more active than the M–X bonds [31]. In experiments, Naguib *et al.* [31] first produced the 2D Ti_3C_2 layer terminated with OH and/or F *via* the 2 h treatment of the conventional MAX phases in aqueous HF. The mixture was centrifuged to separate the solids and then the solids were washed by the deionized water (DI). Consequently, the loosely packed, stacked particles were obtained and were named as the multilayer-, or ML-MXene. In order to get the single- or few-layer MXene, the dimethyl sulphoxide (DMSO) was intercalated with ML-MXene and then the sonication was performed in water to form the 2D MXene [57], as shown in Fig. S1 (Supporting information). However, there also existed some problems for this method, for example, the synthesis of 2D Ti_3C_2 layer was more dependent on the particle size of MAX phase, etching time, reaction temperature, and the concentration of the HF solution [58,59]. The XPS experiment [60] identified that the F-functional group could be substituted by O, so the $Ti_3C_2O_2$ MXene could also be achieved. This strategy is suitable for all the Al-containing MAX phases.

The importance and implications of this synthesis method were that it opened the door for the direct use or *in situ* formation of aqueous HF applied for different sorts of MXenes in experiments. The etchant HF could be utilized for preparing Ti_2CT_x, $TiNbCT_x$, $Ti_3CN_xT_x$, $Ta_4C_3T_x$ [37], Nb_2CT_x, V_2CT_x [61], $Nb_4C_3T_x$, Mo_2CT_x [62], $(Nb_{0.8}Ti_{0.2})_4C_3T_x$, $(Nb_{0.8}Zr_{0.2})_4C_3T_x$ [63], $Zr_3C_2T_x$ [64] and $Hf_3C_2T_x$ [65]. Mo_2C was obtained from the Mo_2Ga_2C phase and the Zr_3C_2 was synthesized by the $Zr_3Al_3C_5$, in which the synthesized transition metal carbides had the formula of $M_nAl_3C_{n+2}$ and $M_n[Al(Si)]_4C_{n+3}$ (M denoted Zr or Hf and n represented 1–3) that were different from the others that prepared from the MAX phase [66]. As we know, the prepared transition metal carbides were

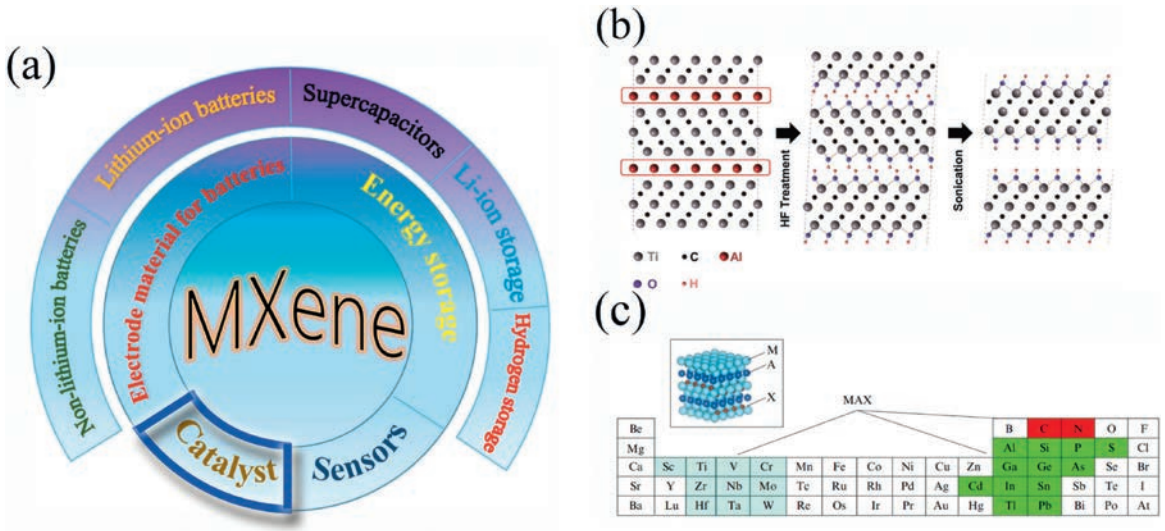

Fig. 1. (a) Schematic of various applications of MXene. Reproduced with permission [49]. Copyright 2018, Wiley-VCH Verlag GmbH & Co. KGaA. (b) Schematic of chemical etching process of Ti_3AlC_2. Copied with permission [31]. Copyright 2011, WILEY-VCH Verlag GmbH & Co. KGaA. (c) The composition elements of MAX phases in the periodic table. Copied with permission [30]. Copyright 2013, Russian Academy of Sciences and Turpion Ltd.

often terminated with different sorts of functional groups, such as O, F or OH, when synthesized by chemical etching. Another proper synthesis method was using the chemical vapor deposition (CVD) to take the place of the wet etching [67], and the remarkable characteristic of this approach was that the preparing process was purer and the obtained 2D MXenes were unterminated [68].

Besides, Halim *et al.* [69] reported the ammonium bifluoride, NH_4HF_2, as a new kind of etchants, to replace the HF solution for a milder reaction conditions. The c lattice parameter of the new etchant produced films was 25% higher than that of the HF-etching films, which was ascribed to the intercalated NH_3 and NH^{4+} species. The prominent advantage of this method was that the NH_4HF_2 was a milder etchant, and it was less hazardous than HF, which leaded to the concomitant intercalation of cations during the whole synthesis process. Afterwards, Ghidiu *et al.* [43] proposed the LiF and HCl mixed solution as a substitute for HF solution to dissolve the Ti_3AlC_2 powders, then heated the content at 40 °C for 45 h, finally washed the sediment to obtain the product. The main advantages of this synthesis method were that the whole etching process was safer, easier, and much faster. Besides, the obtained flakes with large lateral dimensions did not observe the defects in nanometre-size, which reflected the milder nature of LiF + HCl etchant than aqueous HF. Besides, some other fluoride salts, like NaF, KF, CsF, $(CH_3CH_2CH_2CH_2)_4N^+F^-$ and CaF_2 could mix with HCl to replace the HF. Using the H_2SO_4 instead of HCl is also an efficient method to produce MXenes, which shows similar etching behaviors. This synthesis approach could be applied to prepare various kinds of MXenes, including Mo_2CT_x [62], Nb_2CT_x, Ti_2CT_x [43], $Mo_2TiC_2T_x$, $Cr_2TiC_2T_x$, $Mo_2Ti_2C_3T_x$ [70] and $(Nb_{0.8},Zr_{0.2})_4C_3T_x$ [63].

3. MXenes for catalysis

MXenes have been applied for the catalysis, especially in CO oxidation and ORR.

3.1. MXenes as catalysts for CO oxidation

For CO oxidation, MXenes may be the promising candidates to composite with single metal atoms, metal clusters, or metal monolayers to regulate the catalytic activity of the electrocatalysts due to their excellent chemical and physical performances. For example, the Mo_2CO_2 monolayer has been applied as the thermoelectric materials [71], topological insulators [72], energy storage devices [73], catalysts [74] and so on. Besides, Mo_2CO_2 could be synthesized by relatively cheap methods and with high efficiency [73]. Herein, we mainly discuss the catalytic performance of Mo_2CO_2 monolayer in CO oxidation only from the perspective of theoretical aspects because there have been rare experimental investigations in this field. And there are three main types of catalytic mechanisms for CO oxidation, *i.e.*, the Eley-Rideal (ER) mechanism, the Langmuir-Hinshelwood (LH) mechanism, and tri-molecular Eley-Rideal (TER) mechanism. For the traditional ER mechanism, one physisorbed CO molecule approaches the pre-adsorbed O_2 molecule to form the CO_3 intermediate which dissociates later. For the LH mechanism, the CO and O_2 molecules coadsorb on the catalyst before the reaction, and then form the OOCO intermediate, which finally dissociates with the formation of the CO_2 product. And the TER mechanism describes that one O_2 molecule can be activated by two CO molecules together.

There have been rare experimental researches studied the CO oxidation in the recent years. For the theoretical investigations of CO oxidation, Cheng *et al.* [1] demonstrated that the Mo_2CO_2 MXene could serve as an excellent substrate material of the SACs, as shown in Fig. 2. The CO oxidation on the Pd SAC supported on the defective Mo_2CO_2 monolayer with an oxygen vacancy (Pd/O_v-Mo_2CO_2) preferred to occur along the TER mechanism and the energy barrier was 0.49 eV. The CO oxidation catalytic activity of Pd/O_v-Mo_2CO_2 was better than that of the Pd(111) [75] catalyst and approached to that of the Pt(111) [76] catalyst at low CO coverage. Then the authors proceeded to solve the CO poisoning problems and the stability problems of the commercial Pt/C catalysts. The study investigated by Cheng *et al.* [77] demonstrated that the small Cu_3 clusters supported on the Mo_2CO_2 substrate possessed good stability and high catalytic activity for CO oxidation, in which the Cu_3 cluster acted as an electron reservoir to regulate the gaining and losing of electrons, thus promoted the entire reaction, as seen in Fig. 3. The rate-limiting energy barrier was 0.72 eV, which was lower than those of Pt(111) (1.05 eV) [78], Pd(111) (0.93 eV) [79]

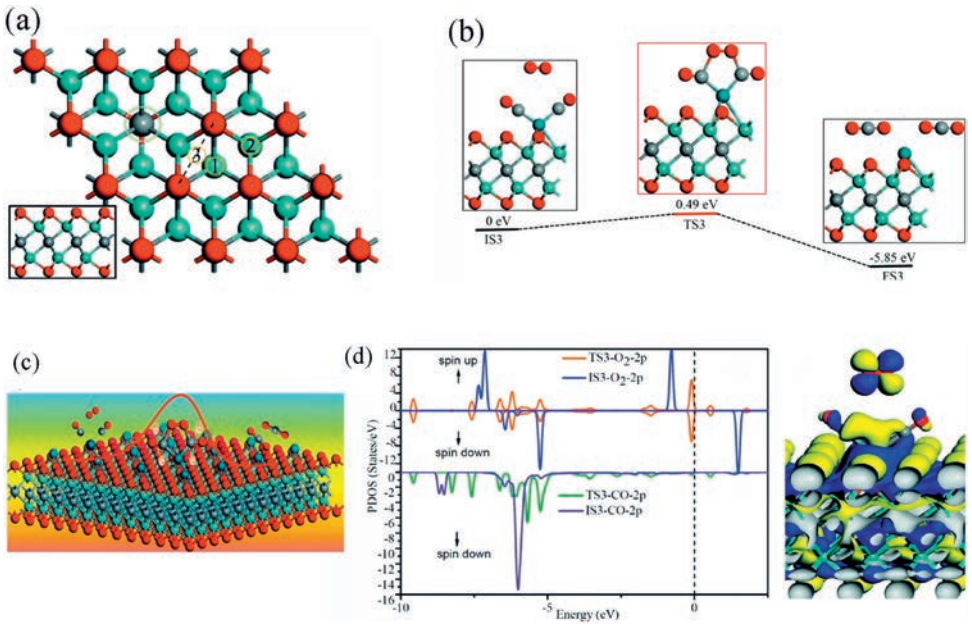

Fig. 2. (a) The top and side views of Mo_2CO_2 monolayer. (b) The catalytic mechanism of CO oxidation on Pd/O_v-Mo_2CO_2 monolayer along TER pathway. (c) The schematic illustration of CO oxidation reaction process *via* TER pathway. (d) Partial density of states (PDOS) of the adsorbed O_2 and CO molecules on the Pd/O_v-Mo_2CO_2, and the front view of LUMO of the free O_2 molecule and the HOMO of two CO molecules on Pd/O_v-Mo_2CO_2. Copied with permission [1]. Copyright 2018, the Royal Society of Chemistry.

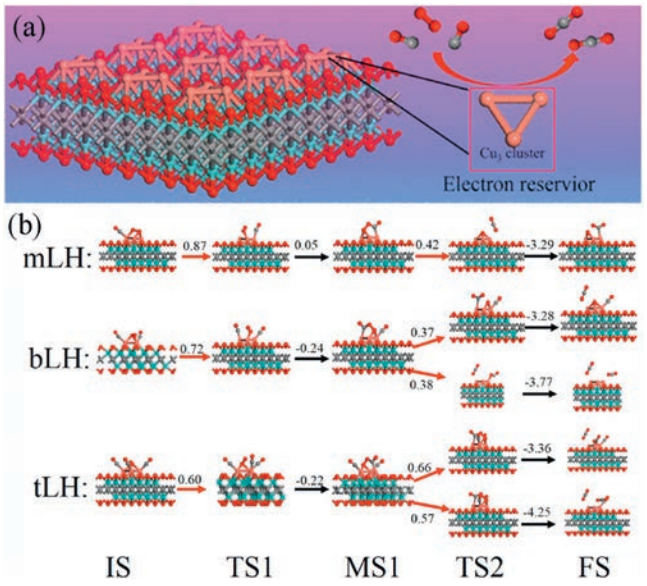

Fig. 3. (a) The schematic of Cu_3 active site of Cu_3/d-Mo_2CO_2 acting as an electron reservoir mediates the CO oxidation reaction process. (b) The reaction pathways (side views) for CO oxidation on Cu_3/d-Mo_2CO_2 *via* the mLH, bLH and tLH mechanisms. Copied with permission [77]. Copyright 2018, American Chemical Society.

and Pd(110) (0.78 eV) [79], indicating the higher reaction activity. Further, the authors continued to explore the common nature of the catalytic materials based on the former investigation [1] and provided a useful guide for fabricating efficient SACs based on MXenes. The eleven metal atoms from VIII∼IIB groups were doped in the $Mo_2CO_{2-\delta}$ monolayer to form the SACs and three criterias were proposed to screen their stability, anti-oxidation properties, and resistance properties of CO poisoning at low temperature. It was concluded that the Zn-doped $Mo_2CO_{2-\delta}$ is a promising SAC candidate for CO oxidation, which may occur along the ER mechanism with the energy barrier of 0.15 eV [80]. The reaction barrier of Zn-doped $Mo_2CO_{2-\delta}$ was much lower than those of the Pt(111) catalyst (1.05 eV) [78], and Pd(111) catalyst (0.93 eV) [79], indicating the higher catalytic performance of Zn-doped $Mo_2CO_{2-\delta}$. In addition, the authors [81] also found that the composite with the Ag monolayer supported on Mo_2C MXene not only possessed high ORR activity, but also exhibited high resistance for CO poisoning. The large surface electron perturbations caused by the strong metal-support interactions and the moderate binding strength of CO could accelerate the speed of CO oxidation at higher CO concentration, thus purified the hydrogen fuel. Besides, the CO oxidation occurred on the Ti anchored Ti_2CO_2 MXene (Ti/Ti_2CO_2) also exhibited outstanding performance along the ER mechanism as that investigated by Zhang *et al.* [33]. The reaction barrier of CO was 0.25 eV, which was lower than that of Pt/FeO_x [82], exhibiting the high catalytic activity for Ti/Ti_2CO_2 in low-temperature CO oxidation, as shown in Fig. S2 (Supporting information). Therefore, the MXenes can serve as the support with outstanding catalytic performance for CO oxidation for the single atom, single cluster or the monolayer of transition metals.

3.2. MXenes as catalysts for ORR

Developing the stable cathode catalysts with exceedingly high electrocatalytic ORR activity and durability has proven to be a major challenge. Recently, Wang and coworkers [83] reported the carbon supported Pt(111) catalyst under peptide assistance with enhanced activity and stability, in which the mass activity and specific activity were about two times greater than that of the commercial Pt/C catalysts, but the durability is still poor because of the weak Pt-C interaction. Thus, searching for efficient corrosion-resistant supporting materials of the electrocatalysts suitable for both the acid and alkaline media is greatly desired. Generally, there are two possible reaction pathways for ORR: The dissociation mechanism and association mechanism. For the dissociation mechanism, the adsorbed O_2 molecule dissociates into two separated O* species. For the association mechanism, the adsorbed O_2 is hydrogenated with one proton and an electron to form the OOH* species.

Lin *et al.* [84] found that the freestanding ultrathin 2D Ti_3C_2 nanosheets with the thickness of 0.5–2.0 nm exhibited outstanding ORR activity and stability in the alkaline condition in experiments. The much more positive ORR onset potential of ∼0.85 V compared with the reversible hydrogen electrode (RHE) and the current density of 2.3 mA/cm^2 suggested the high ORR catalytic efficiency of the as-prepared ultrathin Ti_3C_2 nanosheets (noted as SL Ti_3C_2) as the ORR catalyst. And the Tafel slope of SL Ti_3C_2 was 64 mV/dec in 0.1 mol/L KOH, which was close to that of the commercial Pt/C catalysts as 74 mV/dec [85]. When MXenes hybridized with other dopants, their ORR activity may be enhanced. For example, Xie *et al.* [86] experimentally demonstrated that the Pt nanoparticles and $Ti_3C_2T_2$ hybrid presented the improved durability and enhanced ORR activity compared with the traditional Pt/C catalysts. The initial half-wave potentials of Pt/$Ti_3C_2X_2$ was 0.847 V at 1600 rpm in O_2-saturated 0.1 mol/L $HClO_4$, which was higher than that of the traditional Pt/C catalysts of 0.834 V [86], indicating that the ORR catalytic efficiency of Pt/$Ti_3C_2X_2$ was higher than that of Pt/C catalysts. Wen *et al.* [87] reported a FeNC/MXene hybrid nanosheets whose electrocatalytic performance and durability were excellent with the half-wave potential of 25 mV higher than the commercial Pt/C catalyst and the 2.6% decay after a 2000 s continuous test. And the FeNC/MXene catalysts exhibited the ORR catalytic efficiency of a 25 mV higher half-wave potential (0.814 V *versus* RHE) than the Pt/C catalysts [87], as shown in the Fig. S3 (Supporting information). Chen *et al.* [88] reported that the half-wave potential of Co-CNT/Ti_3C_2 was 0.82 V and the diffusion-limiting current density was 5.55 mA/cm^2, which was comparable to the Pt/C catalysts [88] with the half-wave potential of 0.82 V and the diffusion-limiting current density of 5.30 mA/cm^2, suggesting the high catalytic efficiency of Co-CNT/Ti_3C_2 as the ORR electrocatalysts. Yang *et al.* [89] demonstrated that the hybrid catalyst of multiwall carbon nanotubes (MWCNTs) decorated with MoS_2 quantum dots (MoS_2 QDs) and $Ti_3C_2T_x$ QDs (denoted as MoS_2QDs@$Ti_3C_2T_x$QDs@MWCNTs) possessed the outstanding ORR catalytic efficiency that the measured Tafel slope of MoS_2QDs@$Ti_3C_2T_x$QDs@MWCNTs catalyst reached 90 mV/dec and the half-wave potential reached 0.75 V, which was comparable to that of commercial Pt/C catalyst [89] with the Tafel slope of 89 mV/dec and the half-wave potential of 0.80 V. Zhang *et al.* [90] successfully synthesized the composite of MXene and Ag nanoparticles and the hybrid system exhibited excellent ORR activity and conductivity along the four-electron transfer process. The MXene/NW-$Ag_{0.9}Ti_{0.1}$ catalyst showed the high catalytic efficiency that the onset potential and the half-wave potential at 1600 rpm were 0.921 V (RHE) and 0.782 V (RHE), which were more positive than that of the traditional Ag/C catalyst with the onset potential of 0.571 V and the half-wave potential of 0.56 V [91]. Aside from the nanoparticles, other promising substitutes for platinum, such as g-C_3N_4 [92], Mn_3O_4 [93] and FeN_4 moiety [94], have been utilized to composite with MXenes to modulate the conductivity, stability, and ORR activity.

Although the experimental researches have investigated lots of MXene-based hybrid catalysts for ORR, the interactions between the MXene substrate and the supporting materials are still not clear, which calls for the continues theoretical studies.

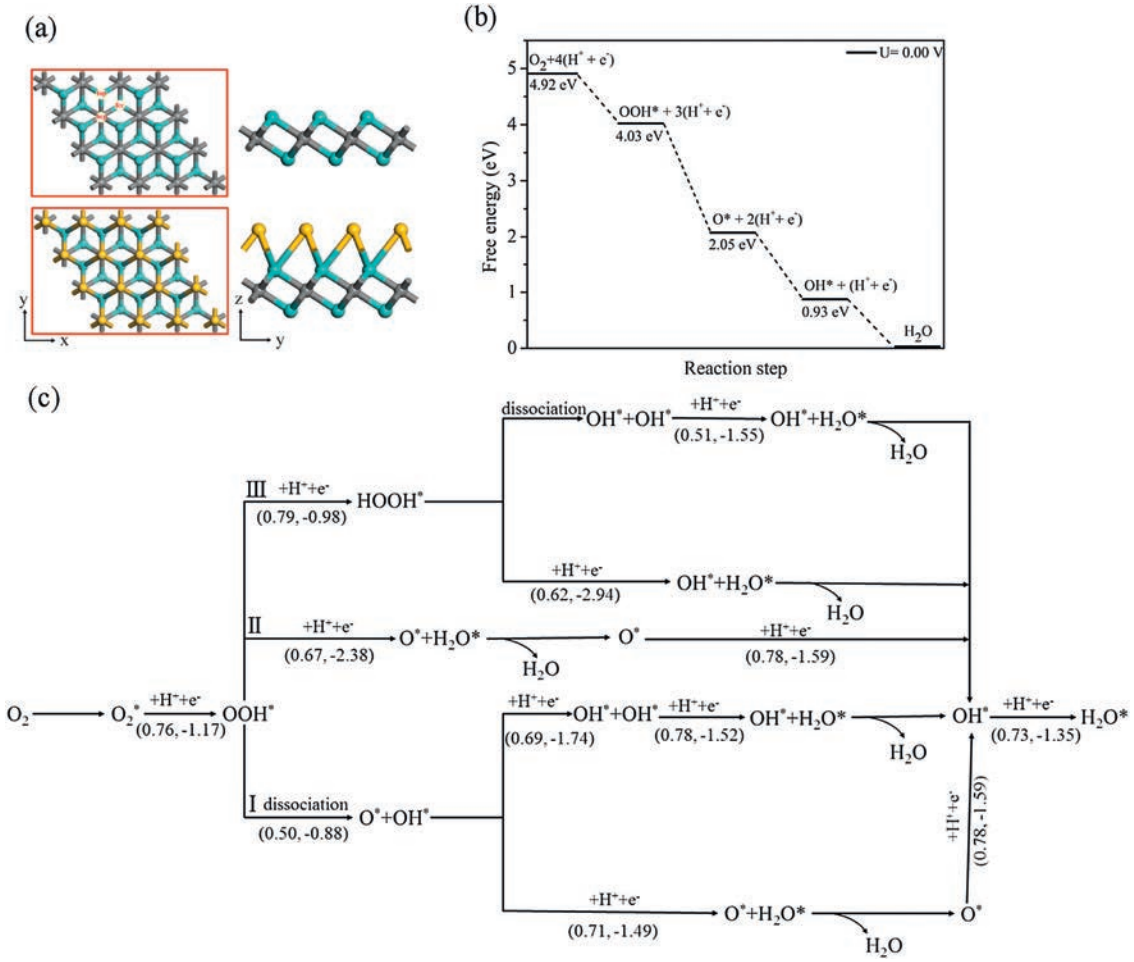

Fig. 4. (a) The top and side views of the pristine Mo_2C and Au monolayer supported Mo_2C (Au_{ML}/Mo_2C). (b) Free-energy diagram for the ORR along the reduction pathway to O* + H_2O on Au_{ML}/Mo_2C at zero electrode potential in acidic medium. (c) The proposed possible reaction pathways for the ORR on Au_{ML}/Mo_2C. Copied with permission [98]. Copyright 2018, IOP Publishing Ltd.

In the theoretical investigations, the bare MXene and the MXene composites show excellent ORR performance for targeted applications, which elucidates the nature of electronic interactions and the exceptionally high catalytic activities. Yang *et al.* [95] reported that the Ti_2CO_2 possessed the lowest ORR/OER/TOT overpotential (TOT potential meant the sum of ORR and OER potentials) among the non-, O-, F-, OH- terminated Ti_2C MXenes, in which the ORR overpotential was 0.10 eV and the OER overpotential was 0.16 eV, suggesting the best catalytic activity for Li-O_2 batteries. Therefore, Ti_2CO_2 showed better ORR and OER catalytic activity than that of the TiC bulk materials, in which the ORR overpotential was 0.69 V and OER overpotential was 1.19 V [96,97]. The MXenes with various dopants also showed excellent performance for ORR. Liu *et al.* [4] investigated the ORR activities of $Ti_{n+1}C_nT_x$ (n = 1–3, T=O or F) and the Pt/v-$Ti_{n+1}C_nT_x$ using the first-principles calculations. The geometries, Bader charges, and the PDOS results manifested that the bonding strength between Ti_2C MXene and the terminated F functional groups was weaker than that between Ti_2C MXene and the O functional groups, suggesting the better ORR performance but low stability of Ti_2CF_2. Cheng *et al.* [98] comprehensively investigated the ORR performance of Cu, Pd, Pt, Ag and Au monolayers decorated Mo_2C MXene using the density functional theory (DFT) calculations and concluded that the Au_{ML}/Mo_2C displayed the best ORR performance, which was comparable or even better than the Pt(111) [99] and Pt(100) [100], as shown in Fig. 4. The outstanding ORR performance along 4-electron process was attributed to the protective layer of Au_{ML} for the antioxidation of Mo_2C substrate and the strong metal-support interactions between Au_{ML} and Mo_2C support, which induced the slightly weaker adsorption strength of gas molecules on Au_{ML}/Mo_2C. Moreover, the DFT simulations investigated by Zhou *et al.* [101] revealed that the V_2C and Mo_2C MXene hybridized with the graphitic sheets showed the outstanding ORR and HER performances. The ORR overpotential of G/V_2C was 0.36 V and its kinetic barrier was 0.2 eV, in which the ORR overpotential of G/V_2C was much lower than that of freestanding N-doped graphene (1.24 V), and even could be an excellent substitute for the benchmark Pt catalyst (0.45 V) [102]. The ΔG_{H^*} of G/V_2C approached to zero and its Tafel reaction barrier was close to 1.3 eV, which was attributed to the strong electronic coupling between the MXene and the hybridized graphitic sheet.

4. Summary and outlook

Since the first MXene, Ti_3C_2, was synthesized in 2011 by selectively etching the Al element from the Ti_3AlC_2 with hydrofluoric acid, some other MXene members in the big family have been explored to investigate their catalytic properties. In this review, the composition, synthesis methods, and the electro-catalysis properties of different kinds of MXenes have been briefly introduced, and we mainly discussed the titanium carbide and molybdenum carbide MXene-based materials used as the catalysts for ORR and CO oxidation. MXenes can serve as the excellent substrate materials to support metal atoms and nanoparticles. This

review gave a preliminary outline on how to regulate the ORR and CO oxidation performance of the MXenes by compositing with metal atoms, metal nanoparticles, metal monolayer or some other 2D materials. The key obstacle of designing the suitable electrocatalysts is that the reaction rate of the crucial reactions has still not emerged a thorough improvement. Some investigations could focus on the ORR and CO oxidation reaction performance of the double transition metal MXenes ($M_1M_2C_2T_x$) and their composites with other 2D nanomaterials, which may be a trend for the future research. Finally, the theoretical studies could be boomingly developed by screening well-performance materials using the high throughput first-principles calculations.

Declaration of competing interest

I would like to declare on behalf of my co-authors that the work described was original research that has not been published previously, and not under consideration for publication elsewhere, in whole or in part. No conflict of interest exits in the submission of this manuscript, and all the authors listed have approved the manuscript that is enclosed.

Acknowledgments

This work was supported by the National Natural Science Foundation of China (Nos. 11874141 and U1804130), Henan Overseas Expertise Introduction Center for Discipline Innovation (No. CXJD2019005).

Appendix A. Supplementary data

Supplementary material related to this article can be found, in the online version, at doi:https://doi.org/10.1016/j.cclet.2019.12.010.

References

[1] C. Cheng, X. Zhang, M. Wang, S. Wang, Z. Yang, Phys. Chem. Chem. Phys. 20 (2018) 3504–3513.
[2] X. Zhang, Z. Zhang, D. Wu, X. Zhao, Z. Zhou, J. Phys. Chem. C 121 (2017) 22895–22900.
[3] Y. Jiao, Y. Zheng, M. Jaroniec, S.Z. Qiao, Chem. Soc. Rev. 44 (2015) 2060–2086.
[4] C.Y. Liu, E.Y. Li, ACS Appl. Mater. Interfaces 11 (2018) 1638–1644.
[5] J. Greeley, I.E. Stephens, A.S. Bondarenko, et al., Nat. Chem. 1 (2009) 552–556.
[6] X. Xie, Y. Xue, L. Li, et al., Nanoscale 6 (2014) 11035–11040.
[7] K.S. Novoselov, A.K. Geim, S.V. Morozov, et al., Science 306 (2004) 666–669.
[8] H. Liu, Y. Du, Y. Deng, P.D. Ye, Chem. Soc. Rev. 44 (2015) 2732–2743.
[9] Y. Lin, T.V. Williams, J.W. Connell, J. Phys. Chem. Lett. 1 (2009) 277–283.
[10] Q. Weng, X. Wang, X. Wang, Y. Bando, D. Golberg, Chem. Soc. Rev. 45 (2016) 3989–4012.
[11] L.H. Li, Y. Chen, Adv. Funct. Mater. 26 (2016) 2594–2608.
[12] X. Huang, Z. Zeng, H. Zhang, Chem. Soc. Rev. 42 (2013) 1934–1946.
[13] C. Tan, H. Zhang, Chem. Soc. Rev. 44 (2015) 2713–2731.
[14] M. Naguib, V.N. Mochalin, M.W. Barsoum, Y. Gogotsi, Adv. Mater. 26 (2014) 992–1005.
[15] C. Wang, F. Lan, Z. He, et al., ChemSusChem 12 (2019) 1576–1590.
[16] G. Zheng, J. Wang, H. Liu, et al., Nanoscale 11 (2019) 18968–18994.
[17] T. Su, Q. Shao, Z. Qin, Z. Guo, Z. Wu, ACS Catal. 8 (2018) 2253–2276.
[18] Y. Zhai, J. Wang, Q. Gao, et al., J. Catal. 377 (2019) 534–542.
[19] P. Yang, L. Yang, Q. Gao, et al., Chem. Commun. (Camb.) 55 (2019) 9011–9014.
[20] B. Lin, Z. Lin, S. Chen, et al., Dalton Trans. 48 (2019) 8279–8287.
[21] Y. Zhang, L. Qian, W. Zhao, et al., J. Electrochem. Soc. 165 (2018) H510–H516.
[22] Z. Li, Y. Wu, Small 15 (2019) e1804736.
[23] D. Deng, K.S. Novoselov, Q. Fu, et al., Nat. Nanotechnol. 11 (2016) 218–230.
[24] Y. Xu, S.X. Jiang, W.J. Yin, et al., Appl. Surf. Sci. 501 (2020) 144199.
[25] C. Wang, V. Murugadoss, J. Kong, et al., Carbon 140 (2018) 696–733.
[26] Y. Zhang, Y. An, L. Wu, et al., J. Mater. Chem. A 7 (2019) 19668–19675.
[27] K. Sun, P. Xie, Z. Wang, et al., Polymer 125 (2017) 50–57.
[28] K. Sun, J. Dong, Z. Wang, et al., J. Phys. Chem. C 123 (2019) 23635–23642.
[29] M. Naguib, Y. Gogotsi, Acc. Chem. Res. 48 (2015) 128–135.
[30] A.L. Ivanovskii, A.N. Enyashin, Russian Chem. Rev. 82 (2013) 735.
[31] M. Naguib, M. Kurtoglu, V. Presser, et al., Adv. Mater. 23 (2011) 4248–4253.
[32] X. Zhang, X. Zhao, D. Wu, Y. Jing, Z. Zhou, Nanoscale 7 (2015) 16020–16025.
[33] X. Zhang, J. Lei, D. Wu, et al., J. Mater. Chem. A 4 (2016) 4871–4876.
[34] Y. Xie, M. Naguib, V.N. Mochalin, et al., J. Am. Chem. Soc. 136 (2014) 6385–6394.
[35] B. Anasori, M.R. Lukatskaya, Y. Gogotsi, Nat. Rev. Mater. 2 (2017) 16098.
[36] P. Urbankowski, B. Anasori, T. Makaryan, et al., Nanoscale 8 (2016) 11385–11391.
[37] M. Naguib, O. Mashtalir, J. Carle, et al., ACS Nano 6 (2012) 1322–1331.
[38] M. Khazaei, M. Arai, T. Sasaki, et al., Adv. Funct. Mater. 23 (2013) 2185–2192.
[39] H. Pan, J. Mater. Chem. A 3 (2015) 21486–21493.
[40] M. Khazaei, M. Arai, T. Sasaki, et al., Phys. Rev. B 92 (2015) 075411.
[41] Q. Tang, Z. Zhou, P. Shen, J. Am. Chem. Soc. 134 (2012) 16909–16916.
[42] M.R. Lukatskaya, O. Mashtalir, C.E. Ren, et al., Science 341 (2013) 1502–1505.
[43] M. Ghidiu, M.R. Lukatskaya, M.Q. Zhao, Y. Gogotsi, M.W. Barsoum, Nature 516 (2014) 78–81.
[44] Q. Zhao, Q. Zhu, J. Miao, et al., Small (2019) e1904293.
[45] N. Sun, Q. Zhu, B. Anasori, et al., Adv. Funct. Mater. (2019) 1906282.
[46] B. Xiao, Y.C. Li, X.F. Yu, J.B. Cheng, Sensor. Actuat. B: Chem. 235 (2016) 103–109.
[47] L. Lorencova, T. Bertok, E. Dosekova, et al., Electrochim. Acta 235 (2017) 471–479.
[48] S.J. Kim, H.J. Koh, C.E. Ren, et al., ACS Nano 12 (2018) 986–993.
[49] X. Li, C. Wang, Y. Cao, G. Wang, Chem. -Asian J. 13 (2018) 2742–2757.
[50] J. Yuan, C. Wang, Y. Liu, P. Wu, W. Zhou, J. Phys. Chem. C 123 (2018) 526–533.
[51] Q. Meng, J. Ma, Y. Zhang, et al., J. Mater. Chem. A 6 (2018) 13652–13660.
[52] M. Fei, R. Lin, Y. Deng, et al., Nanotechnology 29 (2018) 035403.
[53] Y. Cheng, J. Dai, Y. Song, Y. Zhang, ACS Appl. Energy Mater. 2 (2019) 6851–6859.
[54] J.C. Lei, X. Zhang, Z. Zhou, Front. Phys. 10 (2015) 276–286.
[55] V.M.H. Ng, H. Huang, K. Zhou, et al., J. Mater. Chem. A 5 (2017) 3039–3068.
[56] Y. Xiao, J.Y. Hwang, Y.K. Sun, J. Mater. Chem. A 4 (2016) 10379–10393.
[57] O. Mashtalir, M. Naguib, V.N. Mochalin, et al., Nat. Commun. 4 (2013) 1716.
[58] O. Mashtalir, M. Naguib, B. Dyatkin, Y. Gogotsi, M.W. Barsoum, Mater. Chem. Phys. 139 (2013) 147–152.
[59] Z. Li, L. Wang, D. Sun, et al., Mater. Sci. Engin. B 191 (2015) 33–40.
[60] Y. Dall'Agnese, M.R. Lukatskaya, K.M. Cook, et al., Electrochem. Commun. 48 (2014) 118–122.
[61] M. Naguib, J. Halim, J. Lu, et al., J. Am. Chem. Soc. 135 (2013) 15966–15969.
[62] J. Halim, S. Kota, M.R. Lukatskaya, et al., Adv. Funct. Mater. 26 (2016) 3118–3127.
[63] J. Yang, M. Naguib, M. Ghidiu, et al., J. Am. Ceram. Soc. 99 (2016) 660–666.
[64] J. Zhou, X. Zha, F.Y. Chen, et al., Angew. Chem. Int. Ed. 55 (2016) 5008–5013.
[65] J. Zhou, X. Zha, X. Zhou, et al., ACS Nano 11 (2017) 3841–3850.
[66] Y.C. Zhou, L.F. He, Z.J. Lin, J.Y. Wang, J. Eur. Ceram. Soc. 33 (2013) 2831–2865.
[67] Y. Gogotsi, Nat. Mater. 14 (2015) 1079–1080.
[68] C. Zhan, W. Sun, Y. Xie, D.E. Jiang, P.R.C. Kent, ACS Appl. Mater. Interfaces 11 (2019) 24885–24905.
[69] J. Halim, M.R. Lukatskaya, K.M. Cook, et al., Chem. Mater. 26 (2014) 2374–2381.
[70] B. Anasori, Y. Xie, M. Beidaghi, et al., ACS Nano 9 (2015) 9507–9516.
[71] M. Khazaei, M. Arai, T. Sasaki, M. Estili, Y. Sakka, Phys. Chem. Chem. Phys. 16 (2014) 7841–7849.
[72] H. Weng, A. Ranjbar, Y. Liang, et al., Phys. Rev. B 92 (2015) 075436.
[73] R. Meshkian, L.Å. Näslund, J. Halim, et al., Scripta Mater. 108 (2015) 147–150.
[74] Z.W. Seh, K.D. Fredrickson, B. Anasori, et al., ACS Energy Lett. 1 (2016) 589–594.
[75] T. Engel, G. Ertl, J. Chem. Phys. 69 (1978) 1267.
[76] A. Eichler, J. Hafner, Phys. Rev. B 59 (1999) 5960.
[77] C. Cheng, X. Zhang, Z. Yang, Z. Zhou, ACS Appl. Mater. Interfaces 10 (2018) 32903–32912.
[78] A. Alavi, P. Hu, T. Deutsch, P.L. Silvestrelli, J. Hutter, Phys. Rev. Lett. 80 (1998) 3650.
[79] C. Zhang, P. Hu, J. Am. Chem. Soc. 123 (2001) 1166–1172.
[80] C. Cheng, X. Zhang, Z. Yang, K. Hermansson, Adv. Theory Simulations 2 (2019) 1900006.
[81] C. Cheng, X. Zhang, Z. Yang, J. Phys. Condens. Matter. 31 (2019) 215201.
[82] B. Qiao, A. Wang, X. Yang, et al., Nat. Chem. 3 (2011) 634–641.
[83] W. Wang, Z. Wang, M. Yang, C.J. Zhong, C.J. Liu, Nano Energy 25 (2016) 26–33.
[84] H. Lin, L. Chen, X. Lu, et al., Sci. China Mater. 62 (2018) 662–670.
[85] G. Ren, X. Lu, Y. Li, et al., ACS Appl. Mater. Interfaces 8 (2016) 4118–4125.
[86] X. Xie, S. Chen, W. Ding, Y. Nie, Z. Wei, Chem. Commun. 49 (2013) 10112.
[87] Y. Wen, C. Ma, Z. Wei, X. Zhu, Z. Li, RSC Adv. 9 (2019) 13424–13430.
[88] J. Chen, X. Yuan, F. Lyu, et al., J. Mater. Chem. A 7 (2019) 1281–1286.
[89] X. Yang, Q. Jia, F. Duan, et al., Appl. Surf. Sci. 464 (2019) 78–87.
[90] Z. Zhang, H. Li, G. Zou, et al., ACS Sustain. Chem. Engin. 4 (2016) 6763–6771.
[91] E.J. Lim, S.M. Choi, M.H. Seo, et al., Electrochem. Commun. 28 (2013) 100–103.
[92] X. Yu, W. Yin, T. Wang, Y. Zhang, Langmuir 35 (2019) 2909–2916.
[93] Q. Xue, Z. Pei, Y. Huang, et al., J. Mater. Chem. A 5 (2017) 20818–20823.
[94] Z. Li, Z. Zhuang, F. Lv, et al., Adv. Mater. 30 (2018) 1803220.
[95] Y. Yang, M. Yao, X. Wang, H. Huang, J. Phys. Chem. C 123 (2019) 17466–17471.
[96] Y. Yang, Y. Qin, X. Xue, et al., J. Phys. Chem. C 122 (2018) 17812–17819.
[97] Y. Yang, Y. Wang, M. Yao, X. Wang, H. Huang, Phys. Chem. Chem. Phys. 20 (2018) 30231–30238.
[98] C. Cheng, X. Zhang, Z. Fu, Z. Yang, J. Phys. Condens. Matter. 30 (2018) 475201.
[99] Z. Duan, G. Wang, Phys. Chem. Chem. Phys. 13 (2011) 20178–20187.
[100] Z. Duan, G. Wang, J. Phys. Chem. C 117 (2013) 6284–6292.
[101] S. Zhou, X. Yang, W. Pei, N. Liu, J. Zhao, Nanoscale 10 (2018) 10876–10883.
[102] J.K. Nørskov, J. Rossmeisl, A. Logadottir, et al., J. Phys. Chem. B 108 (2004) 17886–17892.